Electronic Supplementary Material (ESI) for Journal of Materials Chemistry A.


Electronic Supplementary Material (ESI) for Journal of Materials Chemistry A.
This journal is © The Royal Society of Chemistry 2019

# A safe and fast-charging lithium-ion battery anode using MXene supported $Li_3VO_4$

Yanghang Huang,[†a] Haochen Yang,[†a] Yi Zhang,[*ab] Yamin Zhang,[a] Yutong Wu,[a] Mengkun Tian,[c] Peng Chen,[a] Robert Trout,[a] Yao Ma,[a] Tzuho Wu,[a] Yuping Wu[*b] and Nian Liu[*a]

[a] School of Chemical and Biomolecular Engineering, Georgia Institute of Technology, Atlanta, GA 30332, USA

[b] College of Energy and Institute for Electrochemical Energy Storage, Nanjing Tech University, Nanjing 211816, Jiangsu Province, China

[c] Institute for Electronics and Nanotechnology, Georgia Institute of Technology, Atlanta, GA 30332, USA

† These authors contributed equally to this work.

Email: nian.liu@chbe.gatech.edu

zhangy@njtech.edu.cn

wuyp@njtech.edu.cn

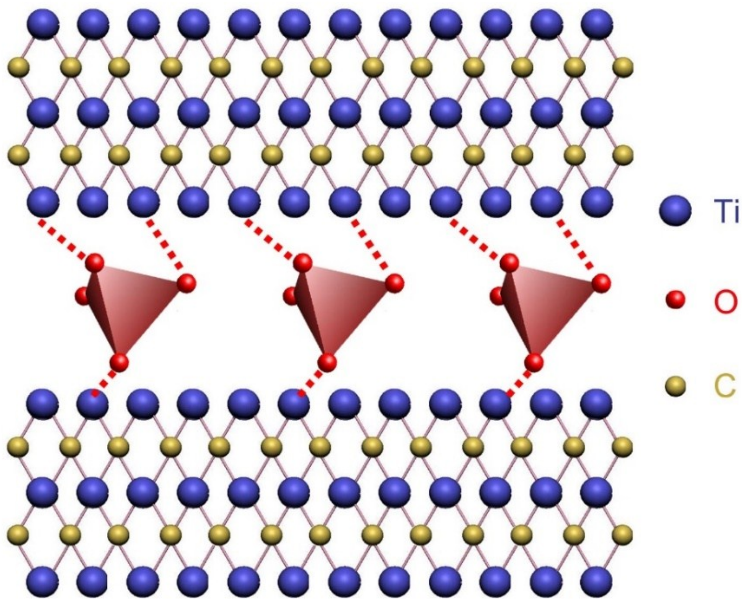


**Figure S1**. The binding between Ti atomic of MXene and O atomic of LVO.

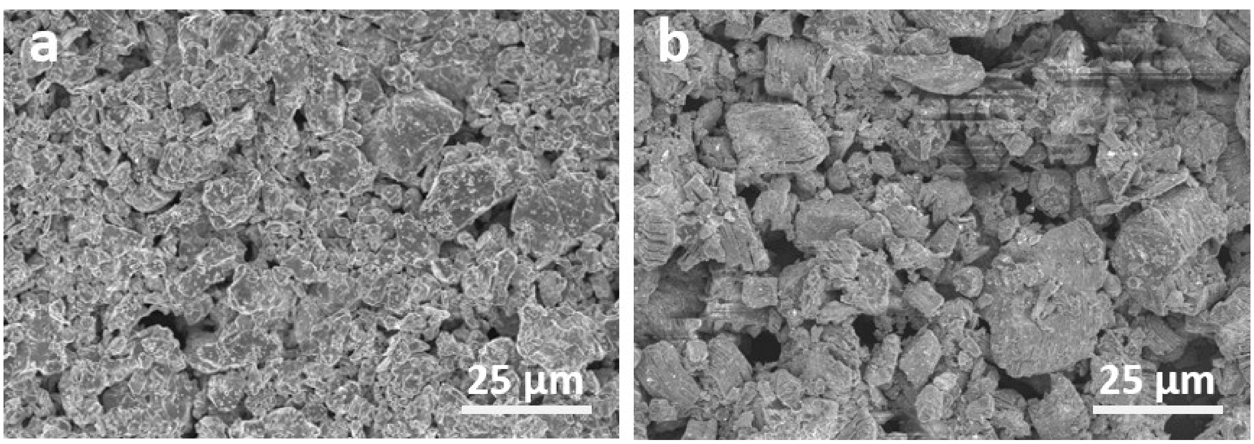


**Figure S2.** SEM images of (a) MAX and (b) MXene.

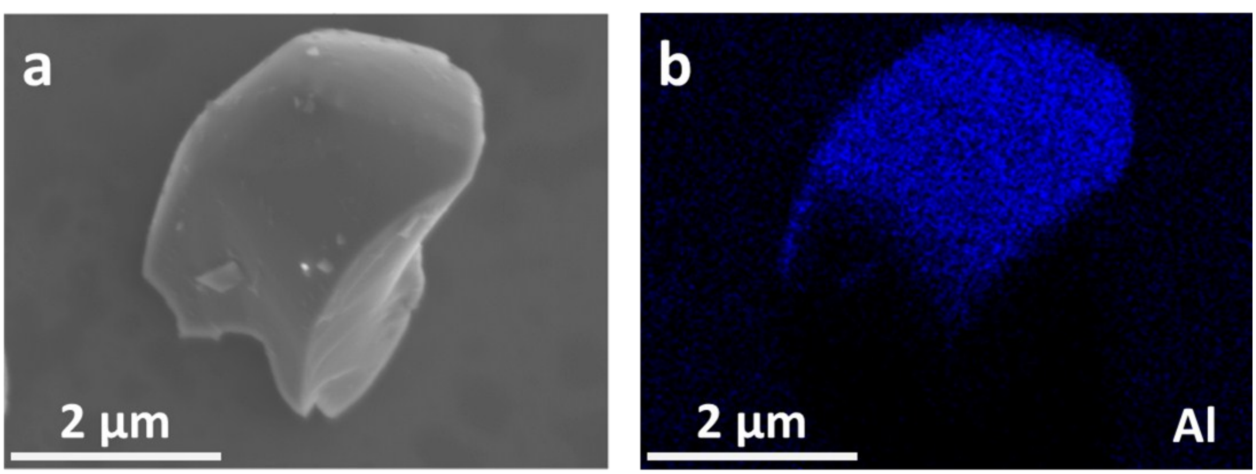


**Figure S3.** (a) SEM image and (b) EDX mapping of MAX.

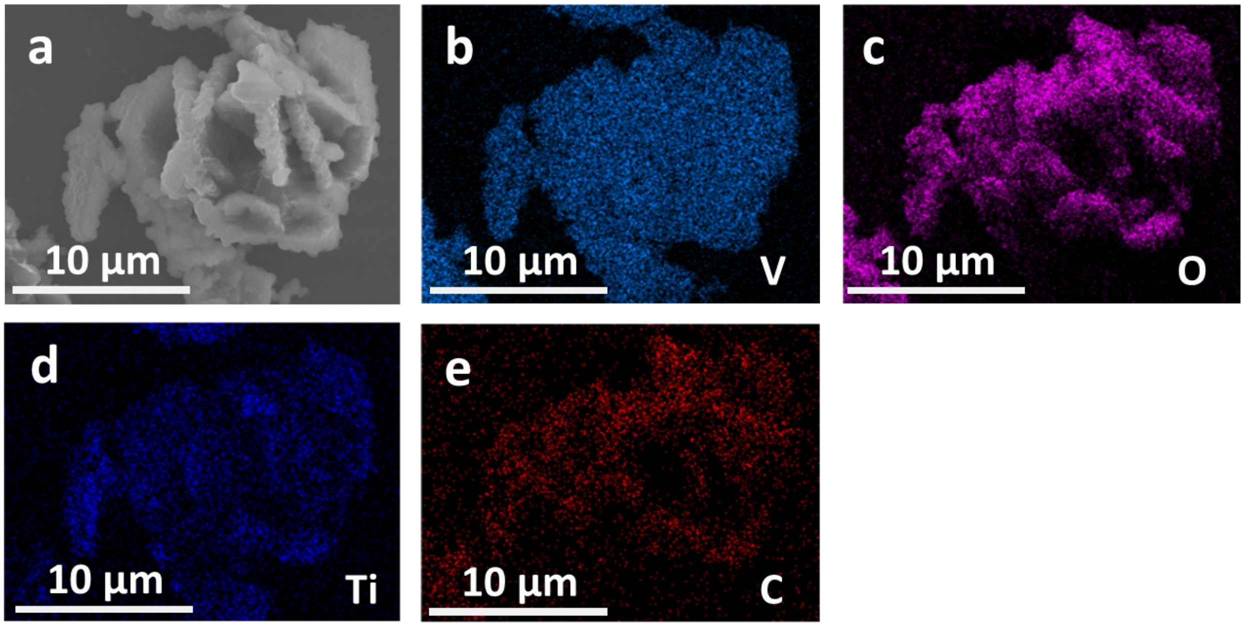


**Figure S4.** (a) SEM image and corresponding EDX mapping of (b) V, (c) O, (d) Ti and (e) C in the LVO/$Ti_3C_2T_x$ MXene composite.

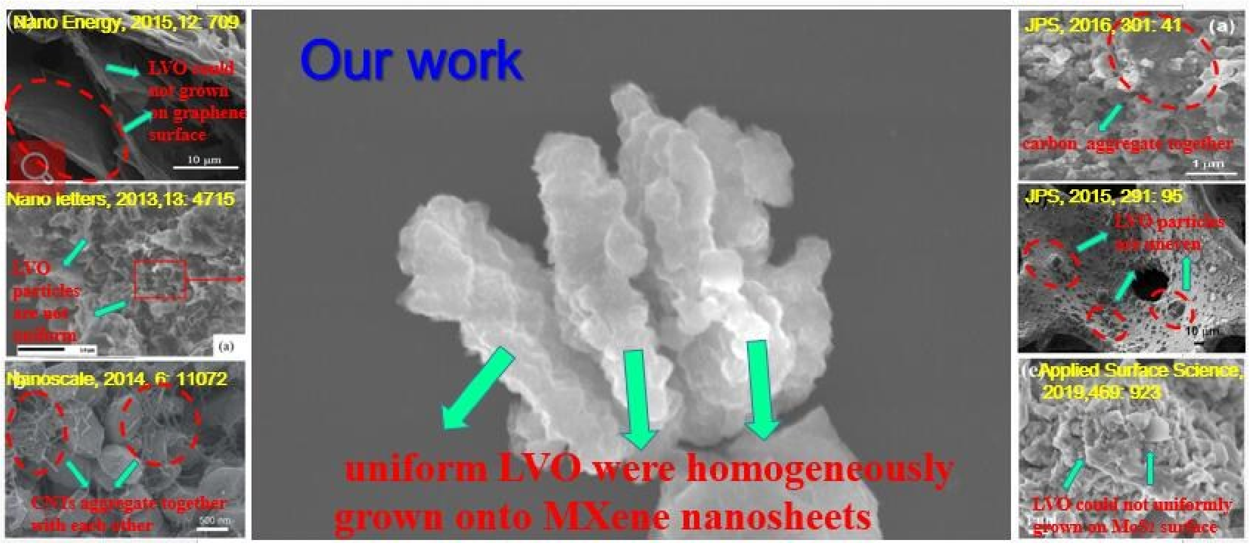


**Figure S5**. The morphology of LVO composites from past works (six images on the two sides) and our work (center). The intrinsic electrical conductivity of LVO is low. Compositing LVO with conductive materials such as graphene[1, 2], carbon nanotubes[3], graphite[4], Ni[5] and $MoS_2$[6] have been tried before. However, most of the past works still contain a large amount of LVO clusters on the surface of MXene nanosheets (**Figure S5**). In our work, the uniform LVO nanoparticles were uniformly grown onto MXene nanosheets. We believe the reason is that MXene is composed of metal and carbon, and the metal ion termination gives it strong affinity with LVO, which allows the uniform growth of LVO on MXene, as illustrated in **Figure S1**.

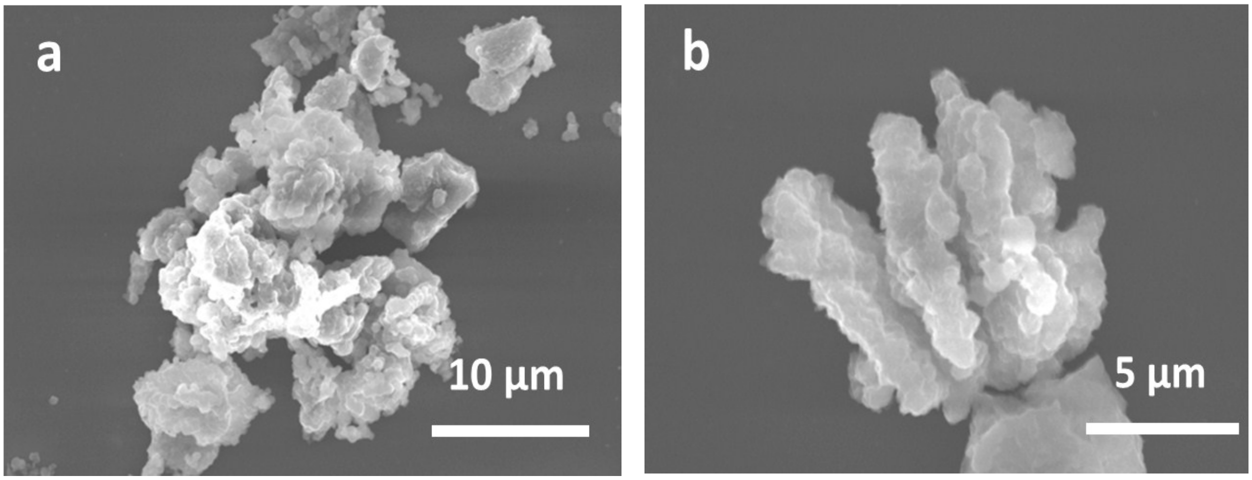


**Figure S6.** SEM images of LVO/$Ti_3C_2T_x$ MXene composite after 10 minutes sonication.

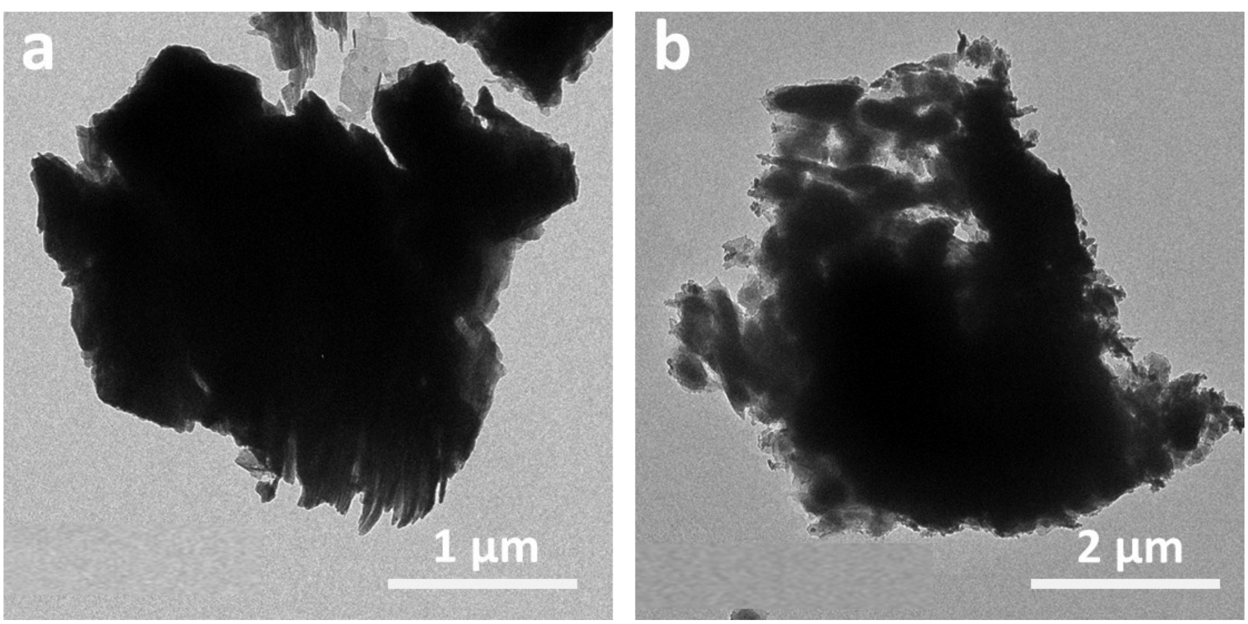


**Figure S7.** Low-magnification TEM images of (a) $Ti_3C_2T_x$ MXene and (b) LVO/$Ti_3C_2T_x$ MXene.

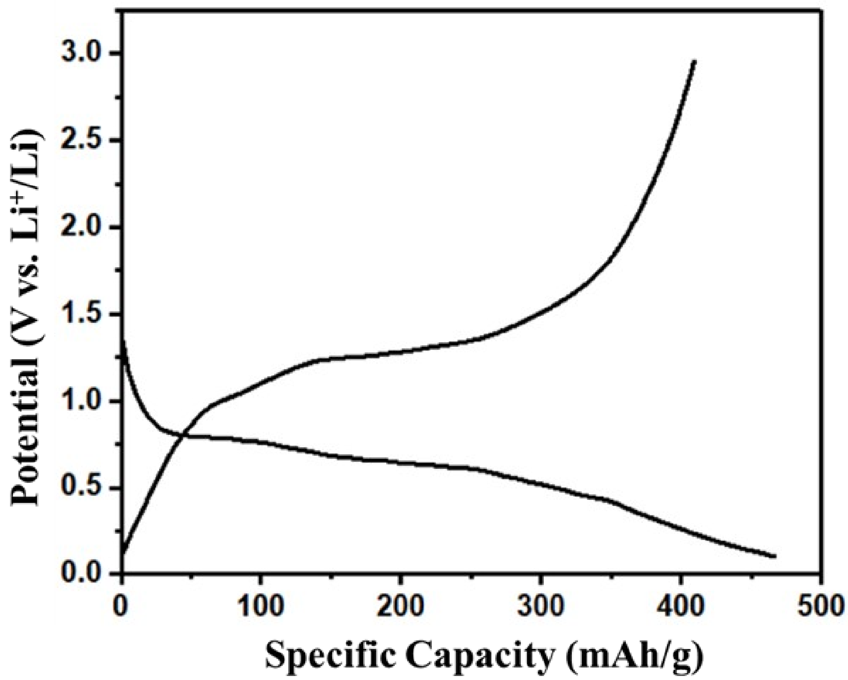


**Figure S8**. The first cycle charge/discharge curves of LVO/$Ti_3C_2T_x$ MXene composite anode in the voltage window of 0.1 V to 3.0 V at 0.1 C.

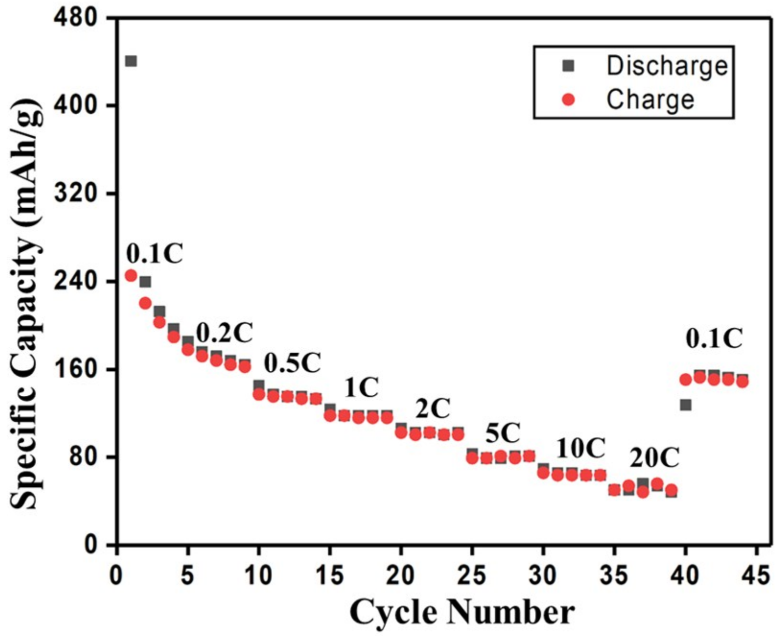


**Figure S9**. Rate performance of pure $Ti_3C_2T_x$ MXene.

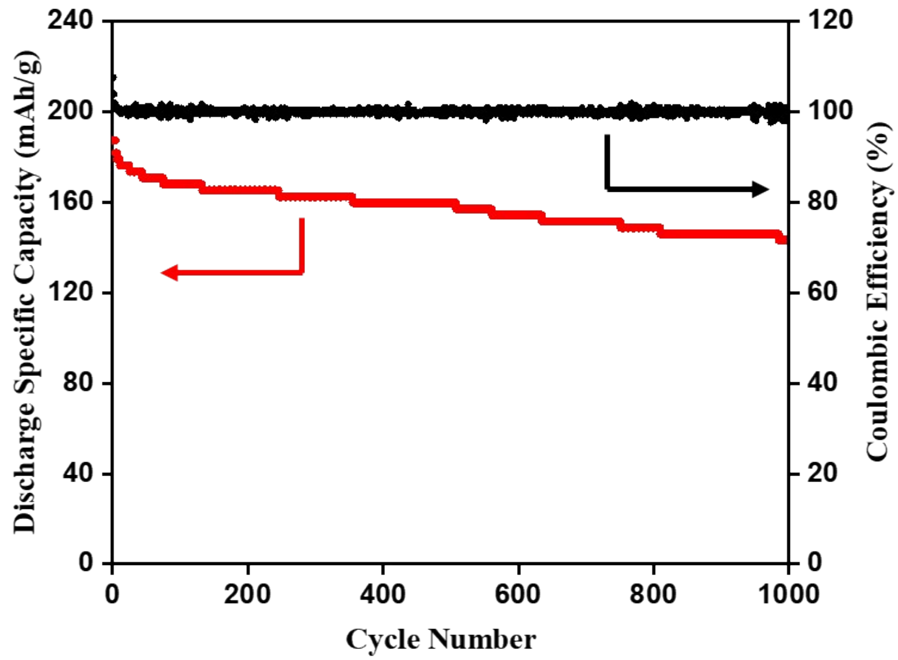


**Figure S10**. Discharge specific capacity and Coulombic efficiency of LVO/$Ti_3C_2Tx$ MXene anode

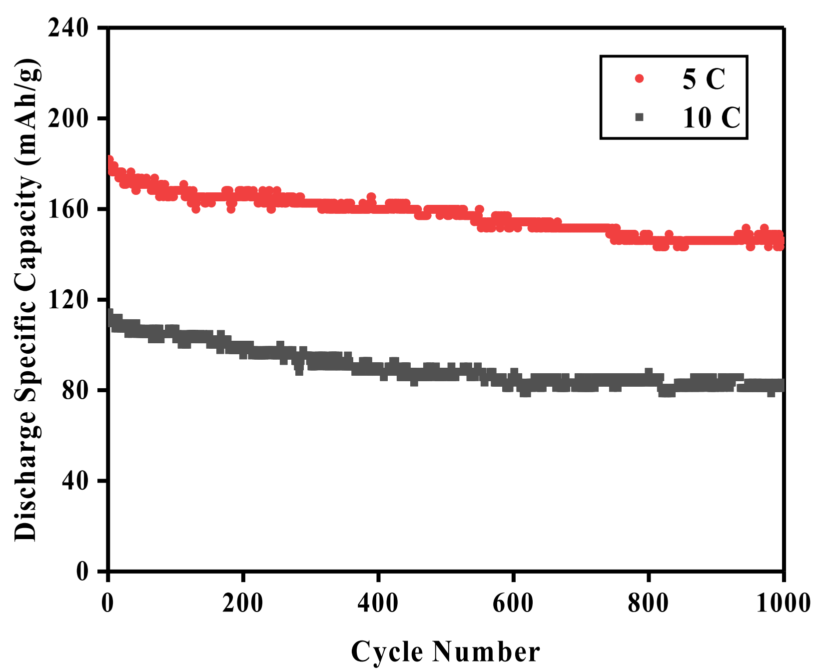


cycled at 5 C.

**Figure S11**. Capacity retention of LVO/$Ti_3C_2Tx$ MXene cycled at 5 C and 10 C.

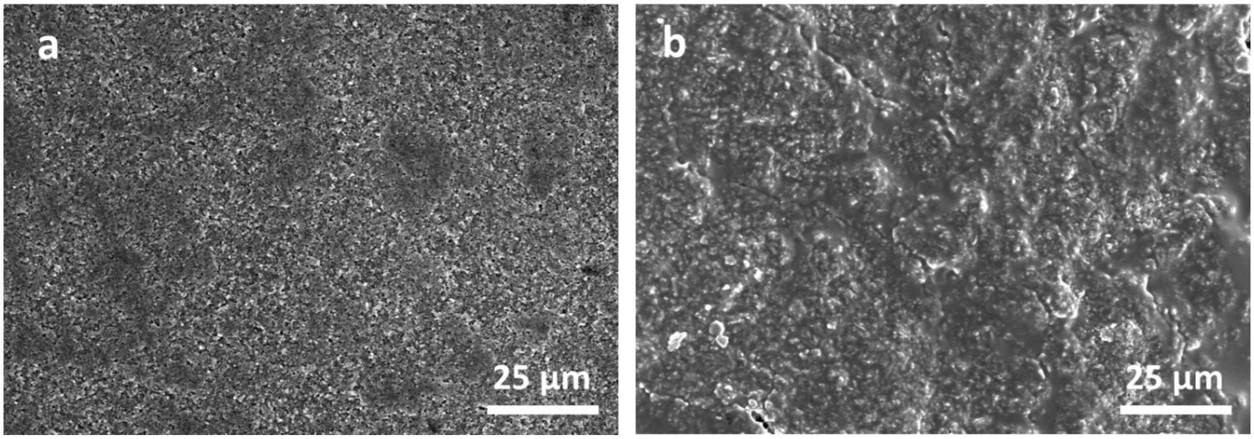


**Figure S12**. SEM images of LVO/$Ti_3C_2Tx$ MXene composite anode (a) before and (b) after 1000 cycles at 5 C.

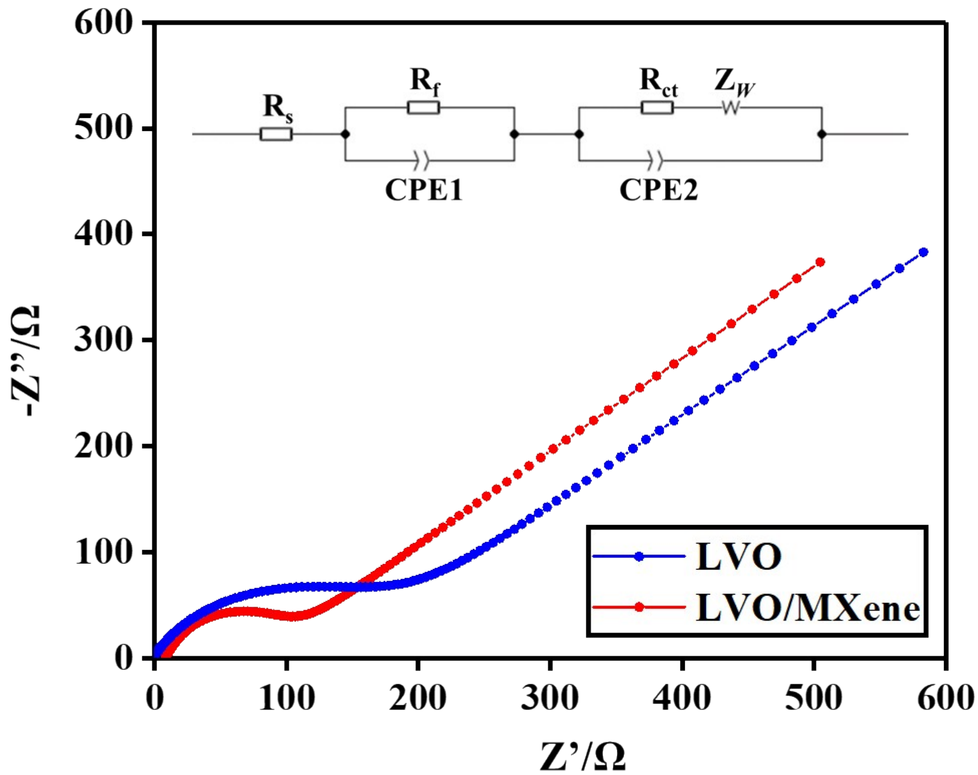


**Figure S13**. Nyquist plots of bare LVO and LVO/$Ti_3C_2Tx$ MXene anodes. Inset: the equivalent circuit model used to simulate the impedance spectrum.

**Table S1**. Comparison of electrical conductivity between MXene, Graphene, Graphene Oxide (GO) and Reduced Graphene Oxide (RGO)

| | Mxene[7] | Graphene[8,9] | GO[10] | RGO[11] |
|---|---|---|---|---|
| Electrical Conductivity (S/m) | **240000** | 500 | Insulation | 1.14 |

**Table S2**. Performance comparison of our LVO/MXene anode with other similar anodes.

| **Anodes** | **High rate capacity** | **High rate cycle stability** | **Reference** |
|---|---|---|---|
| LVO@C[12] | 147 mAh $g^{-1}$ at 0.75C | Not reported | *J Mater Chem A*, **2015**, 3, 11253 |
| O-Deficient LVO[13] | 90 mAh $g^{-1}$ at 5C (20% acetylene black) | No reported | *Adv. Sci.* **2015**, *2, 1500090* |

| | | | |
|---|---|---|---|
| LVO/CNT[14] | 87 mAh $g^{-1}$ at 5C<br>62 mAh $g^{-1}$ at 10C | Not reported | *ACS Nano* **2016**, 10, 5398 |
| LVO nanoparticle[15] | 107 mAh $g^{-1}$ at 5C<br>(20% acetylene black) | Not reported | *ACS Appl Mater Inter,* **2016**, 8, 23739 |
| LVO-Rod[16] | 150 mAh $g^{-1}$ at 5C<br>110 mAh $g^{-1}$ at 5C | Not provided | *J. Mater. Chem. A,* **2018**, 6, 456 |
| LVO@C nanofibers[17] | 141 mAh $g^{-1}$ at 5C<br>98 mAh $g^{-1}$ at 10C | Not reported | *Sci. Bull.* **2017**, 62, 1081 |
| hollow-structured LVO[18] | 140 mAh $g^{-1}$ at 5C<br>110 mAh $g^{-1}$ at 10C | 100 mAh $g^{-1}$ after 1000 cycles at 10C<br>(20% carbon black) | *Chem. Eur. J.* **2014**, 20, 5608-5612 |
| LVO nanoparticle[19] | 86 mAh $g^{-1}$ at 10C | 71 mAh $g^{-1}$ after 1000 cycles at 10C<br>(20% carbon black) | *J. Solid State Electro - chem.* **2017**, 21, 2547 |
| LVO@GNs[20] | 250 mAh $g^{-1}$ at 5C<br>210 mAh $g^{-1}$ at 10C | 163 mAh $g^{-1}$ after 5000 cycles at 5C | *Chem. Commun.* **2015**, 51, 229-231 |
| LVO@ N-doped C[21] | 141 mAh $g^{-1}$ at 5C<br>60 mAh $g^{-1}$ at 10C | 103 mAh $g^{-1}$ after 1000 cycles at 10C<br>(20% acetylene black) | *J. Alloy. Comp.* **2018**, 767, 657 |
| **LVO/MXene** | **187 mAh $g^{-1}$ at 5C**<br>**114 mAh $g^{-1}$ at 10C** | **146 mAh $g^{-1}$ after 1000 cycles at 5C**<br>**81 mAh $g^{-1}$ after 1000 cycles at 10C**<br>**(only 10% carbon black)** | **This work** |

## Reference:


1. J. Liu, P.-J. Lu, S. Liang, W. Wang, M. Lei, S. Tang and Q. Yang, *Nano Energy*, 2015, **12**, 709
2. Y. Shi, J.-Z. Wang, S.-L. Chou, D. Wexler, H.-J. Li, K. Ozawa, H.-K. Liu and Y.-P. Wu, *Nano Lett.*, 2013, **13**, 4715–4720
3. Q. Li, J. Sheng, Q.Wei, Q. An, X. Wei, P. Zhang, and L.Mai. *Nanoscale* 2014, **19**, 11072-11077.
4. J. Zhang, S.Ni, J. Ma, X. Yang, and L.Zhang. *Journal of Power Sources* 2016, **301**, 41-46.
5. S. Ni, J. Zhang, X. Lv, X. Yang, and L. Zhang. *Journal of Power Sources* 2015, **291**, 95-101.
6. M. Zhang, X. Bai, Y. Liu, Y.Zhang, Y.Wu, D. Cui, Y. Liu, L. Wang, B Li, and X. Tao. *Applied Surface Science* 2019, **469**, 923-932.
7. Z. Ling, C. E. Ren, M.-Q. Zhao, J. Yang, J. M. Giammarco, J. Qiu, M. W. Barsoum and Y. Gogotsi, *Proc. Natl. Acad. Sci.*, 2014, **111**, 16676–16681.
8. H. D. Pham, V. H. Pham, T. V. Cuong, T. D. Nguyen-Phan, J. S. Chung, E. W. Shin and S. Kim, *Chem. Commun.*, 2011, **47**, 9672–9674.

9. B. Marinho, M. Ghislandi, E. Tkalya, C. E. Koning and G. de With, *Powder Technol.*, 2012, **221**, 351–358.
10. S. Stankovich, D. A. Dikin, R. D. Piner, K. A. Kohlhaas, A. Kleinhammes, Y. Jia, Y. Wu, S. T. Nguyen and R. S. Ruoff, *Carbon N. Y.*, 2007, **45**, 1558–1565.
11. B.-S. Kong, H.-W. Yoo and H.-T. Jung, *Langmuir*, 2009, **25**, 11008–11013.
12. G. Shao, L. Gan, Y. Ma, H. Li and T. Zhai, *J. Mater. Chem. A*, 2015, **3**, 11253–11260
13. L. Chen, X. L. Jiang, N. N. Wang, J. Yue, Y. T. Qian and J. Yang, *Adv. Sci.*, 2015, **9**, 1500090
14. E. Iwama, N. Kawabata, N. Nishio, K. Kisu, J. Miyamoto, W. Naoi, P. Rozier, P. Simon and K. Naoi, *ACS Nano*, 2016, **10**, 5398–540
15. L. L. Zhou, S. Y. Shen, X. Peng, L. N. Wu, Q. Wang, C. H. Shen, T. T. Tu, L. Huang, J. T. Li and S. G. Sun, *ACS Appl. Mater. Interfaces*, 2016, **8**, 23739
16. G. Yang, B. Zhang, J. Feng, Y. Lu, Z. Wang, V. Aravindan, M. Aravind, J. Liu, M. Srinivasan, Z. Shen and Y. Huang, *J. Mater. Chem. A*, 2018, **6**, 456–463.
17. G. Shao, H. Li, R. Qin, J. Hou, Z. Zheng and T. Zhai, *Sci. Bull.*, 2017, **62**, 1081–1088.
18. Y. Shi, J. Cao, H. D. Abruna, H. J. Li, H. K. Liu, D. Wexler, J. Z. Wang and Y. P. Wu, *Chem.–Eur. J.*, 2014, **20**, 5608
19. S. Chou, D. Wexler, Z. Zhang, H. Li, Y. Shi, H. D. Abruña, J. Wang, J. Gao, H. Liu, J. Wang, Y. Zhang, Y. Wu and L. Liu, *J. Solid State Electrochem.*, 2016, **21**, 2547–2553.
20. Z. Jian, M. Zheng, Y. Liang, X. Zhang, S. Gheytani, Y. Lan, Y. Shi and Y. Yao, *Chem. Commun.*, 2015, **51**, 229
21. H. Park, W. Jae and J. Kim, *J. Alloys Compd.*, 2018, **767**, 657–665.